ORIGINAL PAPER

Density functional study on the sensing properties of nano-sized BeO tube toward H$_2$S

Nastaran Ahmadaghaei · Maziar Noei

Abstract Using density functional calculations, we have investigated the adsorption of a H$_2$S molecule on the pristine and Si-doped BeO nanotubes (BeONT). It was found that the H$_2$S molecule is physically adsorbed on the pristine BeONT with adsorption energies ranging from 3.0 to 4.2 kcal/mol. Substituting a Be or O atom of the tube by Si increases the adsorption energy to 6.9–17.2 kcal/mol. We found that substituting an O atom by Si makes the electronic properties of the BeONT strongly sensitive to the H$_2$S molecule. Therefore, the process of Si doping provides a good strategy for improving the sensitivity of BeONT to toxic H$_2$S, which cannot be trapped and detected by the pristine BeONT. Also, the emitted electron current density from the Si$_O$–BeONT will be significantly increased after the H$_2$S adsorption.

Keywords Sensor · DFT · Nanotubes · Hydrogen sulfide

Introduction

Since the discovery of the carbon nanotubes (CNTs) by Iijima in 1991 [1], a lot of work has been done on new nanoscale tubular materials because of their great potentials in technological applications [2–7]. It was postulated that other compounds that form laminar graphite-like

N. Ahmadaghaei
Department of Chemistry, Shahre-Rey Branch, Islamic Azad University, Tehran, Iran

M. Noei (✉)
Department of Chemistry, Mahshahr Branch, Islamic Azad University, Mahshahr, Iran
e-mail: noeimaziar@gmail.com

structures could also form nanotubes. Nanotubes of BN, AlN and SiC have been synthesized successfully [8–10]. Theoretical studies have shown that CNTs could be either metallic or semiconducting, depending on the radii and chiralities. The electronic characteristics in non-carbon solids depend strongly on the type of intra-particle chemical bonding. This is in contrast to CNTs where nanotubes are either metallic or semiconducting, depending on their tubular diameter and chirality [11]. Nanotubes exhibit potential applications in gas adsorbents and sensors because of their unique properties such as high surface to volume ratio [12–16].

More recently, models of pristine beryllium oxide nanotubes (BeONTs) were proposed and their structural, cohesive and electronic properties were predicted [17, 18]. BeO compound often demonstrates different properties from the counterpart of C, BN and SiC because of the large ionicity of Be–O bond. For example, wurtzite BeO is an insulator with a wide band gap, high melting point, high thermal conductivity and large elastic constants [19]. In addition, compared with CNTs, it was found that the Be-ONTs have a larger band gap which is less dependent on the chirality and diameter of tubes [20, 21]. Moreover, the BeONTs adopt interesting mechanical properties, namely their Young's moduli are comparable with those for carbon nanotubes [20]. These advantages give the BeONTs considerable potential for applications in nanoelectronic devices. Meanwhile, other properties of BeONTs have been studied extensively. For example, Gorbunova et al. [18] studied the magnetism in BeONTs which is induced by the presence of carbon impurities. He et al. [22] studied the optical absorption spectra and the effect of uniaxial strain along the tube axis of BeONTs using first-principle density functional theory and proposed that the BeONTs can be used as anisotropic devices and sensors of

photoelectrons. Seif and Zahedi [23] calculated the electronic structures and the quadrupole coupling constants in the pristine and carbon-doped BeONTs. Like those of the CNTs, BNNTs and SiCNTs, the modifications of doping and adsorption can effectively tune BeONTs electronic structure and expand their applications.

Hydrogen sulfide (H$_2$S) is a toxic and malodorous gas emanating mainly from gasoline, natural gases and city sewage. It is detrimental to human body and the environment [24]. According to the safety standards established by American Conference of Government Industrial Hygienists, the threshold limit value defined for H$_2$S is 10 ppm. Meanwhile, the type of oil or natural gas is correlative with the concentration of H$_2$S [25]. The oil or natural gas mines can be found depending on the concentration of H$_2$S. Therefore, effective methods to monitor formaldehyde have been demanded for atmospheric environmental measurement and control [26]. People have been looking for good materials such as gas sensors with high sensitivity for a long time. Basically, it is expected that the adsorption of gas molecules on the sensors is stable and the changes of the conductivity should be observable. However, most of gases are found physisorbed on suspended intrinsic nanotubes [27–29]. On the contrary, the dopants and defects in nanotubes can strongly enhance the adsorption of molecules [30, 31], indicating that doped atoms and defects play important roles in the applications of them. In the present work, within the density functional theory (DFT) framework, we are interested in the following: (1) whether there is a possibility of BeONT serving as a chemical sensor for H$_2$S; (2) if not, can we find a method for improving the sensitivity of BeONT to H$_2$S?

Computational methods

We selected a (4, 4) armchair BeONT consisting of 56 Be and 56 O atoms in which the end atoms have been saturated with hydrogen atoms to reduce the boundary effects. The full geometry optimizations and property calculations on the pristine and Si-doped tubes in the presence and absence of a H$_2$S molecule were performed using three-parameter hybrid generalized gradient approximation with the B3LYP functional and the 6–31G basis set including the d-polarization function (denoted as 6–31G (d)) as implemented in the GAMESS suite of program [32]. GaussSum program [33] has been used to obtain the DOS results. The B3LYP is demonstrated to be a reliable and commonly used theory in the study of different nanostructures [34–36]. Vibrational frequencies were also calculated at the same level of theory to confirm that all the stationary points correspond to true minima on the potential energy surface. We have defined the adsorption energy (E_{ad}) as follows:

$$E_{ad} = E(\text{BeONT}) + E(\text{H}_2\text{S}) - E(\text{H}_2\text{S/BeONT}) + E(\text{BSSE}), \qquad (1)$$

where $E(\text{H}_2\text{S/BeONT})$ is the total energy of the adsorbed H$_2$S molecule on the BeONT surface, and $E(\text{BeONT})$ and $E(\text{H}_2\text{S})$ are the total energies of the pristine BeONT and H$_2$S molecules, respectively. $E(\text{BSSE})$ is the basis set superposition error (BSSE) corrected for all interaction energies. The canonical assumption for Fermi level (E_F) is that in a molecule (at $T = 0$ K) it lies approximately in the middle of the highest occupied molecular orbital (HOMO)/lowest unoccupied molecular orbital (LUMO) energy gap (E_g). It is noteworthy to mention that, in fact, what lies in the middle of the E_g is the chemical potential, and since the chemical potential of a free gas of electrons is equal to its Fermi level as traditionally defined, herein, the Fermi level of the considered systems is at the center of the E_g.

Results and discussion

H$_2$S adsorption on the pristine BeONT

As shown in Fig. 1, there are two types of Be–O bonds in BeONT: one is perpendicular to the tube axis and another one that is not in parallel with the tube axis (diagonal). The calculated Be–O bond length and the average diameter of the optimized BeONT were found to be about 1.56 and 5.94 Å, respectively, in accordance with the previously reported values [37]. We also obtained a rippled surface: the cations (Be atoms) move inward the tube, while the anions (O atoms) move outward. This reduces the total energy of the system because the electron–electron
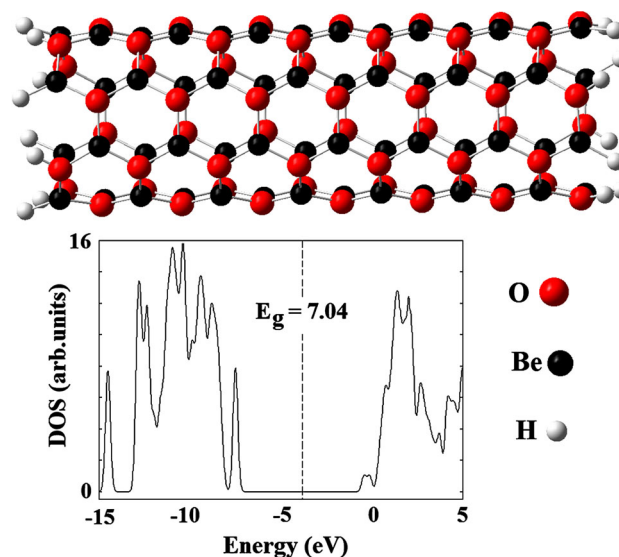

Fig. 1 Partial structure of optimized BeONT and its density of states (DOS). Bonds are in Å

repulsion is lowered, which also agrees reasonably with the previously calculated results [37]. The charge analysis using the based on natural population analysis (NPA) indicates that about 0.502 e charges are transferred from the boron atom to its adjacent nitrogen atoms within the sidewall, indicating the partially ionic character of the Be–O bonds in the sidewall.

In order to obtain the stable configurations of a single adsorbed-H_2S on the tube, various possible initial adsorption geometries including single (hydrogen or sulfur), double (S–H or H–H) and triple H–S–H bonded atoms to Be and O atoms on different adsorption sites were considered. However, only two local minimum structures were obtained after the relaxation process (Fig. 2). More

detailed information about the simulation of the H_2S/BeONT systems including the value of E_{ad}, electronic properties and the charge transfer (Q_T) is listed in Table 1. As shown in Fig. 2a, the H atoms of molecule is close to a O atom of the tube surface with equilibrium distance of 2.14 Å (configuration **A**). The small E_{ad} (about 3.0 kcal/mol) and transferred charge from the tube to the molecule (about 0.092 e) reveal the physical nature of the interaction. The stretching mode of S–H in the adsorbed H_2S occurs at slightly lower frequency of 2,715 cm^{-1} compared with that of the free molecule (2,717 cm^{-1}), confirming the weakness of the interaction.

As shown in Fig. 2b, the most stable configuration of the H_2S/BeONT system is that in which the H_2S molecule can

Fig. 2 Model for stable adsorption of H_2S on the BeONT and its density of state (DOS). Bonds are in Å
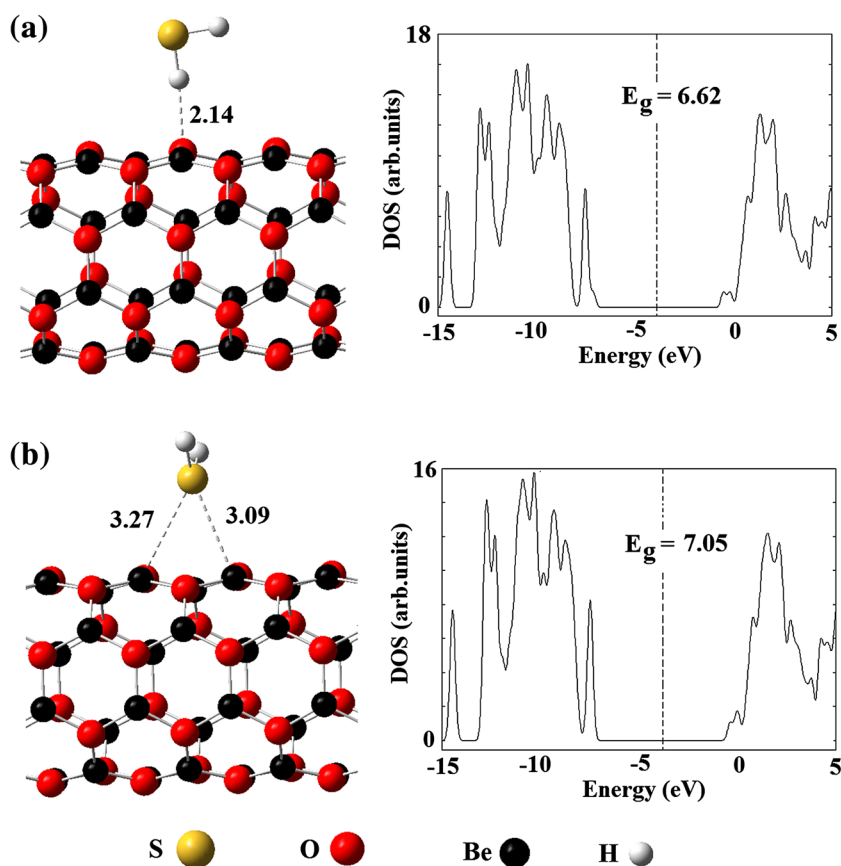
Table 1 Adsorption energy (E_{ad}, kcal/mol), HOMO energies (E_{HOMO}), LUMO energies (E_{LUMO}) and HOMO–LUMO energy gap (E_g), work function (Φ) and Fermi level energy (E_F) of systems (Figs. 1, 2) in eV

Configuration	E_{ad}	Q_T (|e|)[a]	E_{HOMO}	E_F	E_{LUMO}	E_g	ΔE_g (%)[b]	Φ	$\Delta\Phi$[c]
BeONT	–	–	−7.47	−3.95	−0.43	7.04	–	−3.95	–
(A) H_2S/BeONT	3.0	−0.092	−7.12	−3.81	−0.50	6.62	−5.9	−3.81	−3.5
(B) H_2S/BeONT	4.2	−0.103	−7.42	−3.89	−0.37	7.05	+0.1	−3.89	−1.5

[a] Q_T is defined as the total NPA charge on the molecule

[b] Change of E_g of tube after H_2S adsorption

[c] The change of work function of tube after the H_2S adsorption

interact with the tube as bidentate species (**B**, E_{ad} of 4.2 kcal/mol). In this configuration, sulfur atom interacts with two Be atoms with distances 3.09 and 3.27 Å. The adsorption of the H_2S preferably from its S head may be rationalized by the fact that bidentate structure is stabilized by the overlap between the unoccupied s orbital of the Be atom and the occupied $2p_z$ orbital of the S atom of the H_2S. It was also found that the adsorption induces little local structural deformation on both the H_2S molecule and the BeONT. The H–S–H bond angle of the H_2S molecule is slightly increased from 92.8° in free H_2S to 93.4° in the adsorbed state. It is noteworthy to mention that, in contrast to the case of configuration **A**, the stretching mode of S–H (2,689 cm^{-1}) significantly reduced compared with that of the free H_2S.

For the bare BeONT in Fig. 1, it can be concluded that it is a semi-insulator material with a wide E_g of 7.04 eV. To further understand the electronic properties, the DOS plots for the tube after the adsorption of H_2S were compared. By referring to Fig. 2, in the case of configuration **A**, valence level moves to higher energies (−7.12 eV) compared with the bare tube (−7.47 eV), while conduction level remains constant, so E_g of BeONT slightly decreased to 6.62 eV for H_2S/BeONT complex because of charge transfer to the tube. In the case of configuration **B**, both conduction and valence levels slightly move to higher energies, so that E_g of the tube increased from 7.04 to 7.05 eV. These changes

in electronic properties are negligible, indicating that BeONT is still a semi-insulator. Thus, we conjecture that the electronic properties of pure BeONT are insensitive to the H_2S molecule.

H_2S adsorption on the Si-doped BeONT

Furthermore, the effect of substituting Be or O atom of the tube by a Si atom on the electronic properties of the BeONT and also their adsorption behaviors was investigated. As shown in Fig. 3, the geometric structures of the doped BeONTs are dramatically distorted, where the impurity Si projects out of the tube wall because of its larger size, larger than B and N atoms, and its preference to sp^3 hybridization (Fig. 3). The calculated angles and bond lengths on the Si atom center are much smaller and larger than those on the selected Be and O atom center in the pristine BeONT, respectively. This geometrical distortion results in an important change in the electronic properties of the nanotube. Here, we denote the Si impurity as Si_{Be} or Si_O, implying that it substitutes a Be atom or an O atom in the pristine BeONT.

For the electron-rich Si_{Be}–BeONT, the Si atom doping causes a dangling valence for the Si atom and induces the BeONT into an electron-rich system. So, as shown in Fig. 3a, a new donor-like impurity state appears near the conduction band edge, and at the same time a new peak

Fig. 3 Partial structure of optimized (**a**) Si_{Be}–BeONT, (**b**) Si_O–BeONT and their density of states (DOS) plot. Bonds are in Å
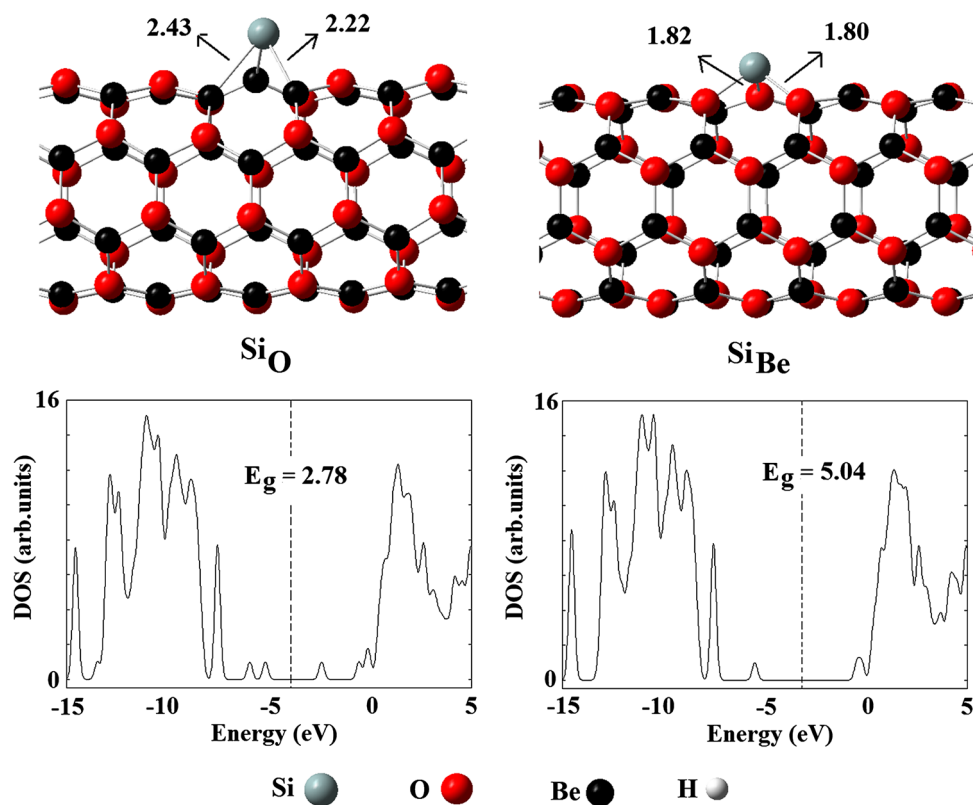
occurs on the top of the valence band, thereby reducing the E_g value of the system to 5.04 eV. Similarly, for the electron-deficient Si_O–BeONT system, the E_g value is decreased to 2.78 eV, and a new local energy level occurs on the top of the valence band (Fig. 3b), which may act as a capture center for atoms or molecules which cannot be trapped by the pristine BeONT.

Subsequently, we have explored H_2S adsorption on the tube by locating the molecule above the Si atom with different initial orientations. We identified one distinct adsorptive configuration of H_2S for each Si-doped tube, as shown in Fig. 4. Configuration **P** (H_2S/Si_O–BeONT complex) gives rise to an E_{ad} of 17.0 kcal/mol, which is more than the E_{ad} values for the configuration **R** (H_2S/Si_{Be}–BeONT complex, 6.9 kcal/mol). On comparison, H_2S adsorption on Si-doped BeONT is energetically more favorable than that on the pristine tube. In configuration **P**, sulfur atom of H_2S was located on the top of Si atom with the corresponding bond length of 2.25 Å (Fig. 4P). In Table 2, we have summarized the results for E_{ad}, Q_T and E_g for H_2S adsorption on the Si-doped tube. Larger charge transfer (0.205 e) and larger E_{ad} between the Si_O–BeONT and the molecule indicate that the doping of Si improves the reactivity of the tube toward the molecule, which is in agreement with the usual mechanism proposed for such binding: the H_2S binds at the exposed Si_O atom which is electron-deficient (unlike Si_{Be}) and can receive electrons

from the lone pair orbitals of sulfur. In other words, unlike beryllium atoms, the hybridization of the Si atom is close to sp^3, and it can have a coordination number of 4. This site which can accept more electrons is referred to as ''Lewis acid sites'' (and conversely, S atom of molecule is termed as ''Lewis base''). Why is the reaction of H_2S with Si_O–BeONT more favorable than that with the Si_{Be}–BeONT? To answer this question, we investigated frontier molecular orbital (FMO) analysis of the doped tube. Figure 5 shows that after Si doping, LUMO of the Si_O–BeONT locates mainly on the doped area (unlike Si_{Be}–BeONT). It is well known the HOMO of H_2S, located on S atom, tends to donate electrons to the LUMO. Therefore, its interaction with Si_O–BeONT will be much stronger than with Si_{Be}–BeONT.

In order to show a qualitative feature of the nature of the interaction between H_2S and doped Si and O atoms in more detail, we performed the Morokuma analysis [38] on the complexes **A** and **P**. Our results unveil that the nature of the both interactions is mainly electrostatic rather than covalent. Also, the interaction in the configuration **A** has more electrostatic character in comparison with that of the configuration **P**. Additionally, we have explored the effect of basis set on the obtained results. The dispersion term to the total energy may give a non-negligible contribution, especially in the calculation of the H_2S physisorption. Therefore, we have repeated all of the E_{ad} calculations,

Fig. 4 Models for stable adsorption of H_2S/Si-doped BeONTs and their density of states (DOS) plot. Bonds are in Å
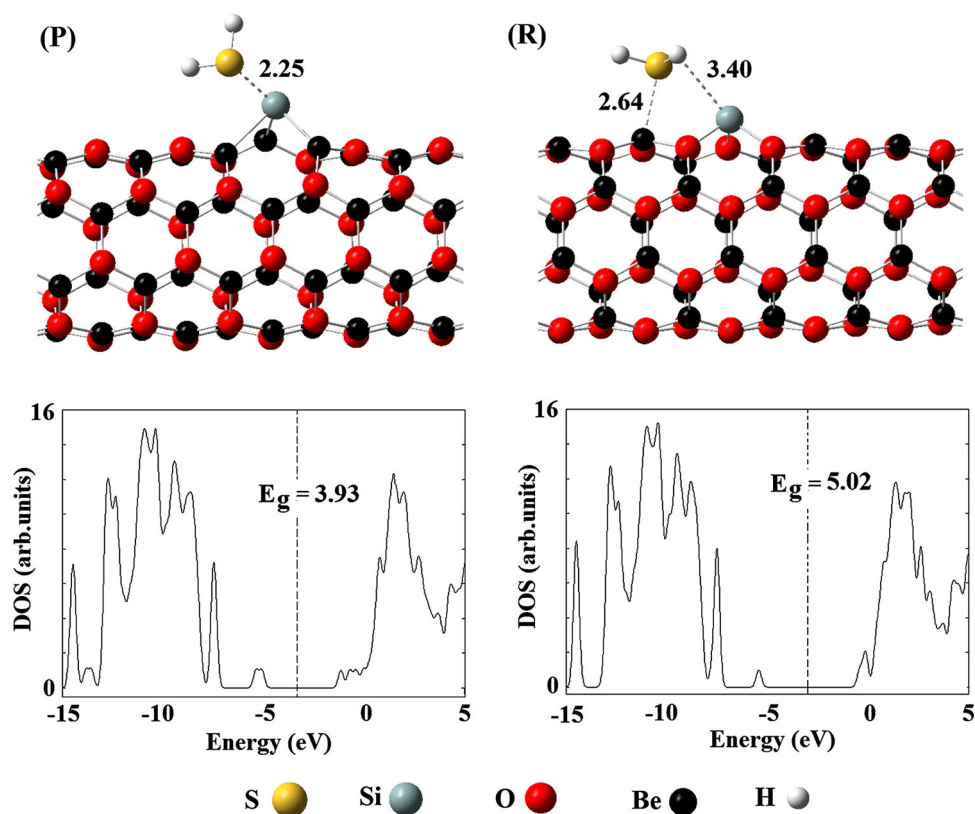
Table 2 Adsorption energy (E_{ad}, kcal/mol), HOMO energies (E_{HOMO}), LUMO energies (E_{LUMO}) and HOMO–LUMO energy gap (E_g), work function (Φ) and Fermi level energy (E_F) of systems (Figs. 3, 4) in eV

Configuration	E_{ad}	Q_T (lel)[a]	E_{HOMO}	E_F	E_{LUMO}	E_g	ΔE_g (%)[b]	Φ	$\Delta \Phi$[c]
Si_O–BeONT	–	–	−5.18	−3.79	−2.40	2.78	–	3.79	–
(**P**) H_2S/Si_O–BeONT	17.0	+0.205	−5.09	−3.12	−1.16	3.93	+41.3	3.12	−17.6
Si_{Be}–BeONT	–	–	−5.49	−2.97	−0.45	5.04	–	2.97	–
(**R**) H_2S/Si_{Be}–BeONT	6.9	+0.091	−5.43	−2.92	−0.41	5.02	−0.4	2.92	−1.7

[a] Q_T is defined as the total NPA charge on the molecule

[b] Change of E_g of doped tube after H_2S adsorption

[c] The change of work function of doped tube after the H_2S adsorption

Si$_{Be}$

Si$_O$
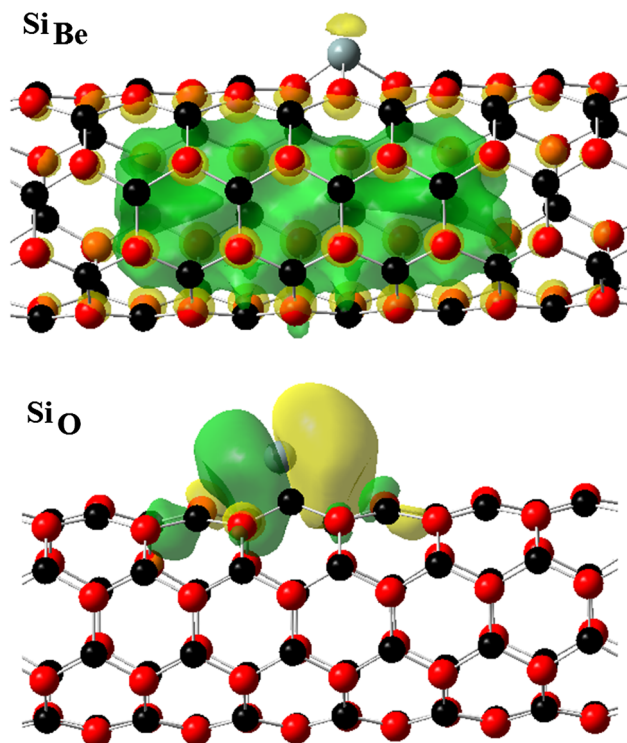
Fig. 5 LUMO profiles of different Si-doped BeONT

using 6–311 + G(d) basis set. The results show that the E_{ad} values of this basis set are about 18.1 and 7.4 kcal/mol for the configurations P and R, respectively, which are slightly larger than those of the 6–31G(d) basis set. E_{ad} values were calculated to be about 4.5 and 5.7 kcal/mol for **P** and **R** configurations, respectively. It indicates that the small E_{ad} values of the configurations **A** and **B** were more influenced by changing the basis set in comparison with those of configurations **P** and **R**.

Calculated DOS plot of H_2S/Si_{Be}–BeONT complex (Fig. 4R) shows that the H_2S adsorption through this configuration has no sensible effect on the electronic properties of the tube so that the E_g of the Si_{Be}–BeONT has a negligible reduction from 5.04 to 5.02 eV. However, DOS plot of the H_2S/Si_O–BeONT complex shows a

considerable change, indicating that the electronic properties of the Si_O–BeONT are sensitive to the toxic H_2S adsorption (Fig. 4P). It is revealed from DOS plot of this configuration that its conduction level shifts significantly to lower energies. As shown in Fig. 4, the E_g value of the Si_O–BeONT is obviously increased from 2.78 to 3.93 eV (by about 41.3 % change) in the adsorbed form, which would result in an electrical conductivity change of the defected sheet according to the following equation:

$$\sigma \propto \exp\left(\frac{-E_g}{2kT}\right), \tag{2}$$

where σ is the electric conductivity and k is the Boltzmann constant [39]. According to the equation, smaller values of E_g at a given temperature lead to larger electric conductivity. Therefore, the predicted substantial decrement of E_g in Si_O–BeONT after the adsorption process induces a change in the electrical conductance of the doped tube. Compared with the bare BeONT, the Si_O–BeONT network would have excellent H_2S detection ability because of its suitable adsorption energy and conductivity.

To further investigate the sensitivity of pristine and Si-doped BeONT, we have studied the changes of work function of systems ascribed to the charge transfer between H_2S and the adsorbents. The work function of a semiconductor is the least amount of energy required to remove an electron from the Fermi level to a point far enough not to feel any influence from the material. The change of work function of an adsorbent after the gas adsorption alters its field emission properties. The readout of gas-induced work function changes via suspended gate field effect devices and has been accepted as a promising technique for the realization of a sensor platform for several years [40]. However, the emitted electron current densities in a vacuum are theoretically described by the following classical equation:

$$j = AT^2\exp(-\Phi/kT), \tag{3}$$

where A is called the Richardson constant (A/m^2), T is the temperature (K) and Φ (eV) is the material's work function.

Work function values were calculated using the following equation:

$$\Phi = E_{\text{inf}} - E_{\text{F}}, \tag{4}$$

where E_{inf} is the electrostatic potential at infinity and E_{F} is the Fermi level energy. In this consideration, the electrostatic potential at infinity is assumed to be zero. The work function changes ($\Delta\Phi$) were calculated by subtracting the work function of the clean tube from that of the corresponding adsorbed system. The results of Table 1 reveal that calculated work function of the pristine BeONT is about 3.95 eV which does not significantly change after the H_2S adsorption. Interestingly, after the H_2S adsorption on the Si_O–BeONT, its work function is considerably decreased from 3.79 to 3.12 eV. A negative work function change (Table 2) may arise from the donation of charge from the H_2S to the tube surface which correlates with an increase in the tube conductance after exposure to the target adsorbate, as has been shown before. However, as can be seen from Eq. 3, the emitted electron current density is exponentially related to the negative value of Φ. Therefore, the emitted electron current density from the Si_O–BeONT will be significantly increased after the H_2S adsorption. So, we believe that Si doping process provides a good strategy for improving the sensitivity of BeONT to toxic H_2S, which cannot be trapped and detected by the pristine BeONT.

Conclusion

The geometric structures and electronic properties of the pristine and different Si-doped BeONT were explored in the presence and absence of an adsorbed H_2S molecule using DFT calculations. In the most stable states, the E_{ad} values corresponding to the adsorption of H_2S on the pristine and Si-doped tube were calculated to be in the range of 3.0–4.2 and 6.9–17.0 kcal/mol, respectively. Interaction of Si_O–BeONT with the molecule is energetically more favorable than pristine BeONT and Si_{Be}–BeONT. HOMO/LUMO energy gap of the Si_O–BeONT is dramatically increased from 2.78 to 3.93 eV after H_2S adsorption. It suggests that Si-doped tube might be electronically sensitive to the presence of H_2S molecule.

References

1. S. Iijima, Nature **354**, 56 (1991)
2. A. Kumar Singh, V. Kumar, Y. Kawazoe, Eur. Phys. J. D **34**, 295 (2005)
3. J. Beheshtian, H. Soleymanabadi, M. Kamfiroozi, A. Ahmadi, J. Mol. Model. **18**, 2343 (2012)
4. Y. Makita, S. Suzuki, H. Kataura, Y. Achiba, Eur. Phys. J. D **34**, 287 (2005)
5. T. Roman, W.A. Diño, H. Nakanishi, H. Kasai, Eur. Phys. J. D **38**, 117 (2006)
6. I. Cabria, M.J. López, J.A. Alonso, Eur. Phys. J. D **34**, 279 (2005)
7. H. Shiroishi, T. Oda, H. Sakashita, N. Fujima, Eur. Phys. J. D **43**, 129 (2007)
8. A. Loiseau, F. Willaime, N. Demoncy, N. Schramcheko, G. Hug, C. Colliex, H. Pascard, Carbon **36**, 743 (1998)
9. T. Taguchi, N. Igawa, H. Yamamoto, S. Jitsukawa, J. Am. Ceram. Soc. **88**, 459 (2005)
10. V. Tondare, C. Balasubramanian, S. Shende, D. Joag, V. Godbole, S. Bhoraskar, M. Bhadhade, Appl. Phys. Lett. **80**, 4813 (2002)
11. N. Hamada, S.I. Sawada, A. Oshiyama, Phys. Rev. Lett. **68**, 1579 (1992)
12. A. Ahmadi, N.L. Hadipour, M. Kamfiroozi, Z. Bagheri, Sens. Actuators B Chem. **161**, 1025 (2012)
13. B.B. Shirvani, M.B. Shirvani, J. Beheshtian, N.L. Hadipour, JICS **8**, S110 (2011)
14. S. Jalili, R. Majidi, JICS **4**, 431 (2007)
15. A. Ahmadi Peyghan, A. Omidvar, N.L. Hadipour, Z. Bagheri, M. Kamfiroozi, Physica E **44**, 1357 (2012)
16. S.H. Mousavipour, R. Chitsazi, JICS **7**, S92 (2010)
17. A. Fathalian, R. Moradian, M. Shahrokhi, Solid State Commun. **156**, 1 (2013)
18. M.A. Gorbunova, I.R. Shein, YuN Makurin, V.V. Ivanovskaya, V.S. Kijko, A.L. Ivanovskii, Physica E **41**, 164 (2008)
19. S. Duman, A. Sutlu, S. Bagcl, H.M. Tutuncu, G.P. Srivastava, J. Appl. Phys. **105**, 033719 (2009)
20. P.B. Sorokin, A.S. Fedorov, L.A. Chernozatonskii, Phys. Solid State **48**, 398 (2006)
21. B. Baumeier, P. Kruger, J. Pollmann, Phys. Rev. B **76**, 085407 (2007)
22. J.G. He, K.C. Wu, R.J. Sa, Q.H. Li, Y.Q. Wei, Appl. Phys. Lett. **97**, 051901 (2010)
23. A. Seif, E. Zahedi, Superlattic. Microstruct. **50**, 539 (2011)
24. E. Sasaoka, S. Hirano, S. Kasaoka, Y. Sakata, Energy Fuels **8**, 1100 (1994)
25. W. Feng, S. Kwon, E. Borguet, R. Vidic, Environ. Sci. Technol. **39**, 9744 (2005)
26. A.D. Mayernick, R. Li, K.M. Dooley, M.J. Janik, J. Phys. Chem. C **115**, 24178 (2011)
27. J. Dai, P. Giannozzi, J. Yuan, Surf. Sci. **603**, 3234 (2009)
28. O. Leenaerts, B. Partoens, F.M. Peeters, Phys. Rev. B **77**, 125416 (2008)
29. T.O. Wehling, K.S. Noveselov, S.V. Morozov, E.E. Vdovin, M.I. Katsnelson, A.K. Geim, A.I. Lichtenstein, Nano Lett. **8**, 173 (2008)
30. J. Dai, J. Yuan, P. Giannozzi, Appl. Phys. Lett. **95**, 232105 (2009)
31. I. Carrillo, E. Rangel, L.F. Magaña, Carbon **47**, 2752 (2009)
32. M.W. Schmidt, K.K. Baldridge, J.A. Boatz, S.T. Elbert, M.S. Gordon, J.H. Jensen, S. Koseki, N. Matsunaga, K.A. Nguyen, S. Su, T.L. Windus, M. Dupuis, J.A. Montgomery, J. Comput. Chem. **14**, 1347 (1993)
33. N. O'Boyle, A. Tenderholt, K. Langner, J. Comput. Chem. **29**, 839 (2008)
34. H. Kökten, Ş. Erkoç, Phys. E **44**, 215 (2011)
35. H.A. Dabbagh, M. Zamani, H. Mortaji, JICS **9**, 205 (2012)
36. L. Chen, C. Xu, X.-F. Zhang, T. Zhou, Physica E **41**, 852 (2009)
37. L.C. Ma, H.S. Zhao, W.J. Yan, J. Magnetism Magn. Mater. **330**, 174 (2013)
38. K. Kitaura, K. Morokuma, Int. J. Quantum Chem. **10**, 325 (1976)
39. S. Li, *Semiconductor physical electronics*, 2nd edn. (Springer, USA, 2006)
40. S. Stegmeier, M. Fleischer, P. Hauptmann, Sens. Actuators B Chem. **148**, 439 (2010)